HIGH INTENSITY 5 eV O-ATOM EXPOSURE

FACILITY FOR MATERIAL DEGRADATION STUDIES

J. B. Cross, L. H. Spangler, M. A. Hoffbauer, and F. A. Archuleta
Los Alamos National Laboratory
Chemistry Division
Los Alamos, NM 87545

Lubert Leger and James Visentine
Lyndon B. Johnson Space Center
Houston, TX 77058

Don E. Hunton
Air Force Geophysics Laboratory
Hanscom Air Force Base, MA 01731

ABSTRACT

An atomic oxygen exposure facility has been developed for studies of material degradation. The goal of these studies is to provide design criteria and information for the manufacture of long life (20 to 30 years) construction materials for use in low earth orbit. The studies that are being undertaken using the facility will provide (1) absolute reaction cross sections for use in engineering design problems, (2) formulations of reaction mechanisms for use in selection of suitable existing materials and design of new more resistant ones, and (3) calibration of flight hardware (mass spectrometers, etc.) in order to directly relate experiments performed in low earth orbit to ground based investigations.

The facility consists of (1) a cw laser sustained discharge source of O-atoms having a variable energy upto 5 eV and an intensity of between 10^{15} -10^{17} O-atoms s^{-1} cm^{-2}, (2) an atomic beam formation and diagnostics system consisting of various stages of differential pumping, a mass spectrometer detector and a time-of-flight analyzer, (3) a spinning rotor viscometer for absolute O-atom flux measurements, and (4) provision for using the system for calibration of actual flight instruments.

INTRODUCTION

The exterior surfaces of spacecraft operating in the low earth orbit (LEO) environment are bombarded with oxygen atoms at an average rate of 10^{15} s^{-1} cm^{-2} and with a collision energy of 5 eV caused by the spacecraft's 8 km/s orbital velocity. In addition to this very reactive species, N_2 (11.5 eV collision energy) and N-atoms are present and collide with these surfaces at fluxes 0.3 and 10^{-3} that of atomic oxygen, respectively.

The reactivities of spacecraft surfaces with the LEO environment which is used to predict surface recession for Space Station materials have been derived by exposing these materials during Shuttle flights of limited duration and low atomic oxygen fluence. These in-flight investigations are important, but the Shuttle is limited in its usefulness in evaluating coating life. For example, even during conditions of maximum solar activity, a 7-day mission at an altitude of 222 km would result in an atomic oxygen fluence of only 1.3×10^{21} atom/cm^2, assuming maximum (normal incidence) exposure. Yet fluences for long-duration missions, such as Space Station, will be in the range of $10^{22} - 10^{23}$ atom/cm^2. Therefore, ground based studies must be conducted to determine the validity of extrapolation to high fluence conditions using reactivities derived from low fluence exposures. To aid in these investigations, a number of atomic oxygen simulation facilities are being developed using various techniques to accurately simulate the LEO environment. The particular facility described here will be used to study: material interaction rates as a function of time, the interaction mechanisms leading to surface recession, the full life ($10^{22}-10^{23}$ atom/cm^2) effects of atomic oxygen on exposed surfaces and protective coatings, and scattering angular distributions and O-atom energy loss both of which will be important parameters in computer modeling of Space Station interaction with the LEO environment. The facility is designed to produce a beam of neutral atomic oxygen at energy levels typical of orbital conditions (5 eV). In addition, it is designed to be capable of producing fluxes in the range of $10^{16}-10^{17}$ atom/s-cm^2, in order to study reactivities at typical Space Station fluences within reasonable periods of time. Assuming an incident flux as high as 5×10^{16} atom/s-cm^2, materials must be exposed for approximately 50 hours to obtain fluence levels typical of Space Station solar inertial surfaces.

The simulation of the LEO environment has focused on the development of intense sources of O-atoms in the energy range of 2 to 10 eV. The limitations of many of these sources can be traced to reactions of the species with the production apparatus and the characteristics of the production methods. For example the source developed by Knuth[1] has been used for the production of atomic oxygen[2] but due to reactions with the electrodes, the oxygen is admitted downstream of the discharge region resulting in a maximum kinetic energy of about 1 eV and an intensity of 3×10^{17} s^{-1} sr^{-1}. Radio frequency discharges[3,4] have been used to produce oxygen atoms with kinetic energies of 0.1 to 1.0 eV and intensities of 10^{17-18} s^{-1} sr^{-1}. The production of high mass kinetic energy species is accomplished by seeding and heating in helium[5] expansions but low mass species (<20 amu) are limited to roughly 1 to 2 eV in kinetic energy using this technique. Charge exchange methods excel at energies >100 eV but suffer from space charge limitations[6] below 10 eV producing beam intensities orders-of-magnitude less than the previously mentioned techniques. Due to the low duty cycle of pulsed beams, techniques using pulsed laser breakdown require peak intensities of 10^3 to 10^4 that of cw beams in order to effectively equal cw time averaged intensities. The plasmas mentioned above are produced by electric fields having a range of frequencies from constant (dc arcs), <1 kHz (ac arcs), 20 to 50 MHz (inductive coupling), and 2.5 GHz (microwaves). These sources require some physical device to support the plasma. Direct current arcs require electrodes, rf plasmas require an induction coil, and microwaves require a resonator or waveguide. Because

rf and microwave source heating occurs by direct plasma-electric field inter-actions characterized by large absorption coefficients with the outer layers of the plasma, these modes of plasma production are characterized by low power den-sity (<200 W cm^{-3}), modest temperatures (<8000 K except for dc arcs - 20,000 K). Power inputs ranging from 15 kW for dc arcs to 100's of watts for rf and micro-wave sources are required.

LASER SUSTAINED PLASMAS

In the early 1970's, it was hypothesized[7,8] and then demonstrated that a free-standing continuous discharge could be produced by focusing the output of a sufficiently powerful cw-CO_2 laser in inert[9] and molecular[10] gases at one atmos-phere or above. The discharge resides near the focus of the laser and operates above the plasma frequency at 30 THz where the electric fields interact with individual electrons and ions to heat the plasma via free-free transitions (inverse Bremsstrahlung).[11] The laser power maintenance threshold depends upon the type of gas, the total pressure, whether the laser beam is horizontal or vertical (convection sweeps the hot gas out of the laser focal volume), the focusability or coherence of the laser beam, and the optical quality of the lens system. For example our work uses a 1-in. focal length ZnSe miniscus AR coated lens operated in the horizontal position with a transverse flow 1.5 kW CO_2 laser. The gases xenon, argon, and neon require 50, 300, and 1300 W, respectively for maintenance of the discharge. Because the focused power of the cw laser is in the range 10^6 to 10^7 W cm^{-2}, several orders of magnitude smaller than typical breakdown thresholds, a high energy external spark is needed to initiate the dis-charge. This can be provided by a conventional spark[12] or as in this work a pulsed CO_2 laser. The primary advantages of the laser sustained discharge in creating energetic atomic beams are the high temperatures produced by the high power densities (10^4 W-cm^{-3}), the ability to sustain the discharge independent of nozzle material, and low total input power. Preliminary results using xenon have been reported in ref. 12.

SOURCE CONSTRUCTION AND OPERATION

A cross-sectional view of the source is shown in figure 1 and consists of two portions, the lens holder and nozzle holder. The 1-in.-diam ZnSe AR coated miniscus lens is clamped to the end of a water-cooled copper tube. Indium gas-kets are used to cushion and seal the lens as well as to provide maximum heat transfer to the copper. A threaded copper clamping ring is tightened onto the lens while heating the lens, holder, and indium to 50 to 70°C. This procedure provides excellent sealing of the lens onto the indium. The nozzle holder is made entirely of copper with all joints being welded rather than brazed. The nozzle body is made from a 3.2-mm platinum rod 3.2-mm long drilled to within 0.76 mm of one end to a diameter of 2.39 mm. The nozzle body is brazed into the end of the nozzle holder and the 0.2-mm- diam nozzle is then electron discharged machined through the 0.76-mm wall. A 3-mm-thick copper wall separates the plati-num nozzle from the water cooling jacket. A double viton O-ring is used to seal the lens and nozzle holders and to locate the lens concentric with the nozzle.

Figure 2 shows the source mounted in the molecular beam scattering apparatus and aligned with both the plasma sustaining cw (maximum power 1.8 kW) and plasma initiating pulsed (0.5 J) CO_2 lasers. The output of the cw laser traverses the length of a 3.2-m laser table and is reflected back and turned 45° to enter the source assembly. Both copper turning mirrors (M1 and M2) are water cooled. The pulsed laser beam is placed nearly coaxial to the cw beam using the set of copper coated glass mirrors (M3, M4, and M5). Initial alignment of the cw, pulsed, and HeNe laser beams is accomplished by burning a pinhole in a 0.1-mm-thick nickel foil using the cw laser and then adjusting the pulsed laser turning mirrors to place it through the same hole. The cw CO_2 laser is then turned off, the mirror M6 placed in the path of the cw beam, and the HeNe laser is aligned to pass through the pinhole.

Final alignment of the cw laser beam with the nozzle is accomplished through operation of the source with argon and optimizing the time-of-flight distributions for maximum velocity by moving the discharge radially using the final turning mirrors M1 and M2 and axially by movement of the ZnSe lens. After initiating and aligning the discharge using argon, other gases are mixed with the argon to obtain radical species with velocities <5 km/s. If velocities greater than 5 km/s are desired, the argon is replaced with neon yielding velocities <10 km/s.

BEAM CHARACTERIZATION

Beam characteristics are depicted in the TOF distributions of figures 3, 4, and 5. The time-of-flight (TOF) analyzer used for these studies consisted of a 12.5-cm-diam disk rotated at 310 Hz with 8 equally spaced 1-mm slots located on its circumference. The TOF analyzer is calibrated using low pressure (200 torr) room temperature expansions of neon, argon, and krypton gases. The ion energy in the quadrupole mass spectrometer detector[12] was found to be 10 eV (25-cm path length) and the neutral flight path length was 19.5 cm. The entrance to the detector was a round 0.152-mm-diam hole. Slots (0.2-mm wide) below each 1-mm slot are used to obtain timing signals from a light bulb and photocell detector. This timing signal was used to control a 256 channel multichannel scaler having a 2-μs dwell time/channel which was used to record the time-of-flight (TOF) spectra. The TOF spectra shown have not been corrected for ion flight times, timing mark offset (12 μs), or instrumental broadening. The reported velocities were obtained by correcting for ion flight times and timing mark offsets but not instrumental broadening.

The calculation of molecular dissociation follows that of Lee,[3]

$$R = N_0/N_{O_2}$$ (1)

$$= (x_D/x_{O_2})/\eta \ (x_{O_2}/x_0)(I_0 - \eta \ I_{O_2})/I_{O_2}$$

$$\% \ dissociation = R/(R+2)$$ (2)

where I_0 and I_{O_2} are the experimentally observed number density signals at mass 16 and 32 with the discharge on, η is the ratio of number densities of mass 16 and 32 with the discharge off, x_D is the dissociative ionization cross section of O_2 to form O^+, $x_D = 0.88$ A^2, and x_i are the ionization cross sections which we have taken to be,

$$x_{O_2} = 1.52 \overset{o}{A}, \text{ and } x_0 = 1.15 \ A^2 \ .$$

Figure 3 shows argon TOF distributions with the discharge off and on. The velocities with the discharge on were calculated to be 4.2 km/s for argon and 6.9 km/s for neon with 'the discharge slightly backed away from the nozzle. Our previous work[12] with xenon predicted that the argon and neon velocities would be 3.6 km/s and 6 km/s, respectively, indicating that a crude estimate of other gas velocities (V_m) can be obtained using the formula[12]

$$V_m = V_{Ar}(40/m)^{1/2} (T_m/T_{Ar})^{1/2} \tag{3}$$

where m is the mass of the carrier gas, the subscript Ar refers to argon, and T_m is the plasma spectroscopic temperature of the carrier gas.[10]

Figures 4 and 5 show TOF spectra for mass 16 and 32 with oxygen mixtures of 40% and 49%, respectively. Essentially 100% dissociation of O_2 into O-atoms was observed with the 40% oxygen argon mixture while a 49% mixture produces 98% dissociation indicating that increasing amounts of oxygen may produce recombination within the nozzle.

The extent of dissociation is highly dependent upon the placement of the discharge within the nozzle; small changes in the radial or axial position can easily produce ratios of O-atoms to O_2 of 50%. Figure 6 shows the effect that a 0.5-mm axial change in the discharge placement in the nozzle has on the gas velocity distribution. As the discharge is moved farther into the nozzle the velocity distribution becomes broader and peaked at higher velocities. The plasma acts as a plug when placed in the nozzle and the initial density (10^{20} cm^{-3}) drops by a factor of roughly 100 to values of 10^{18} to 10^{17} cm^{-3} due to the high temperature of the plasma. At the higher plasma temperature a decrease in the total collision cross section would also be expected.[13] This creates a condition in which the nozzle is operating at a Knudsen number close to unity or in the transition region between hydrodynamic and free molecular flow thus causing a broadening of the velocity distribution. The higher peak velocities are observed because cooler boundary layers in front of the discharge are reduced in intensity.

O-ATOM EXPOSURE FACILITY

Figure 7 shows a diagram of the O-atom beam exposure facility. The beam source is pumped by a 2000 l/s diffusion pump while the two downstream differential pumping chambers are pumped with 500 l/s turbomolecular pumps. The

scattering chamber is equipped with a 1500 1/s turbomolecular pump. A water cooled boron nitride skimmer is used to extract the O-atoms from the expansion and to isolate the nozzle chamber from the first differential pumping stage. A remotely operated straight-through valve on the nozzle chamber allows that chamber to be vented for nozzle replacement without venting the remaining apparatus.

A rotatable quadrupole mass spectrometer detector employing a Brink[14] type ionizer is shown along with the time-of-flight chopper. The three-stage, differentially pumped detector has an angular resolution of 1° and a detection sensitivity of 10^{-4}, i.e., one ion is produced for every 10,000 neutrals entering the ionizer.

The port opposite the nozzle source houses a spinning rotor viscometer[15] and calibrated leak which are used for absolute measurements of beam flux. In addition hardware exists for coupling flight mass spectrometers to the system for calibration. The flux (Q) entering the mass spectrometer is calculated from the equation

$$Q = \rho \cdot S$$

where ρ is the absolute number density measured by the calibrated spinning rotor gauge while S is the calculated effusive conductance out the entrance aperture slit of area A_0

$$S = \frac{1}{4} \cdot A_0 \cdot \sqrt{\frac{8\ kT}{\pi m}}$$

where k = Boltzmann's constant (1.38×10^{-16} ergs molecule^{-1} K^{-1}), T is the wall temperature (Kelvin), and m is the mass of a molecule (grams). Mass spectrometer measurements of O-atoms are then related to this flux Q. Figure 8 shows some representative mass spectra taken with a flight instrument provided by the Air Force Geophysics Laboratory. The primary background is water vapor (10^{-8} torr) and N_2. Lower pressures can be obtained through the use of a liquid nitrogen cryoshroud and mild heating (100°C) of the system.

GAS-SURFACE SCATTERING

Initial results of gas scattering from an uncharacterized nickel surface are presented in figures 9 and 10. The molecular beam apparatus described in ref. 12 was used along with a pseudorandom sequence TOF chopper. The TOF detector is operated at 400 Hz with the multichannel scaler operating with a dwell time/channel of 10 μs. Angular distributions were obtained by modulating the direct beam at 400 Hz with a tuning fork chopper while data was accumulated with a phase locked pulse counter. The TOF chopper was kept in operation during angular distribution measurements. Counting times of 2 min/angle were used for angular distributions and 5 min/angle for TOF acquisition. These initial experiments focused on large incident angle (70°) scattering because of the ease of observing both the direct and scattered beams. The discharge source was operated with a 50% mixture of oxygen and argon with

the axial position of the discharge slightly back of the nozzle (velocity was not optimized). Figure 9 shows strong specular scattering of atomic oxygen over the angular range accessible to the detector indicating predominantly direct scattering with surface residence times on the order of the collision time. Figure 10 shows TOF spectra taken at the specular angle 70° and at 80° from the surface normal for both atomic and molecular oxygen. The data of figure 10 when converted to translational energy indicates that approximately 1/2 the initial beam energy was lost to the solid. The surface was not characterized but most likely consisted of nickel oxide with overlayers of O_2. Further experiments are in progress to obtain angular distributions near the surface normal to determine the extent of energy accommodation and to fully characterize the surface.

CONCLUSION

An O-atom exposure facility has been described which consists of (1) a cw laser sustained discharge source of O-atoms having a variable energy up to 5 eV and an intensity of between 10^{15}-10^{17} O-atoms s^{-1} cm^{-2}, (2) an atomic beam formation and diagnostics system consisting of various stages of differential pumping, mass spectrometer detector and time-of-flight analyzer, (3) a spinning rotor viscometer for absolute O-atom flux measurements, and (4) provision for using the system for calibration of flight instruments.

A new beam source has been described that uses a laser sustained plasma technique for producing high intensity ($>10^{18}$ s^{-1} sr^{-1}) and high translational energy (>2 eV) beams. Data indicates that beam temperatures near the plasma spectroscopic temperature can be obtained and that data from one gas can be used to predict results from others. Atomic oxygen beam energies of 2.5 to 3 eV have been produced with intensities of ~4 x 10^{18} s^{-1} sr^{-1}. Measurements have been taken that show the instrument capable of measuring both the extent of energy equilibration produced by high velocity collisions with engineering type surfaces and nonreactive scattering angular distributions of O-atoms. This type of information along with reaction cross sections will provide the data base for computer modeling of Space Station interactions with LEO environment.

REFERENCES

1. Knuth, E. L.; Winicur, D. H.: J. Chem. Phys. 46 (1967) 4318).
   Knuth, E. L.; Rodgers, W. E.; Young, W. S.: An Arc Heater for Supersonic Molecular Beams, Rev. Sci. Instr. 40 (1969) 1346.

2. Silver, J. A.; Freedman, A.; Kolb, C. E.; Rahbee, A.; Dolan, C. P.: Supersonic Nozzle Beam Source of Atomic Oxygen Produced by Electric Discharge Heating; Rev. Sci. Instr. 53 (1982) 1714.

3. Lee, Y. T.; Ng, C. Y.; Buss, R. J.; Sibener, S. J.: Development of a Supersonic $O(^3P_J)$, $O(^1D_2)$ Atomic Oxygen Nozzle Beam Source, Rev. Sci. Instr. 51 (1980) 167.

4. Grice, R.; Gorry, P. A.: Microwave Discharge Source for the Production of Supersonic Atom and Free Radical Beams, J. Phys. E12 (1979) 857.

5. Campargue, R.: Progress in Overexpanded Supersonic Jets and Skimmed Molecular Beams in Free-Jet Zones of Silence; J. Phys. Chem. 88 (1984) 4466.

6. Ardenne, M. V.: Tabellen der Elektronenphysik, Ionenphysik and Ubermikroskopie., Veb Deutscher Verlag Der Wissenschafter, Berlin (1956), pg. 507.

7. Razier, Y. P.: The Feasibility of an Optical Plasmatron and It's Power Requirements; ZhETF Pis. Red. 11 (1970) 195 [JETP Lett. 11 (1970) 120].

8. Razier, Y. P.: Subsonic Propagation of a Light Spark and Threshold Conditions for Maintenance of a Plasma by Radiation; Zh. Eksp. Teor. Fiz. 58 (1970) 2127 [Sov. Phys. JETP, 31 (1970) 1148].

9. Razier, Y. P.: Laser Induced Discharge Phenomena. Consultants Bureau, New York (1977).

10. Kozlov, G. I.; Kuznetsov, V. A.; Nasyukov, V. A.: Sustained Optical Discharge in Molecular Gases; Zh. Tekh. Fiz., 49 (1979) 2304 [Sov. Phys. Tech. 49 (1979) 1283].

11. Hughes, T. P.: Plasmas and Laser Light. John Wiley, New York (1975).

12. Cross, J. B.; Cremers, D. A.: High Kinetic Energy (1-10 eV) Laser Sustained Neutral Atom Beam Source; Nuc. Instr. and Methods, B13 (1986) 658.

13. Levine, R. D. and Bernstein, R.B.: Molecular Reaction Dynamics; Oxford University Press, New York (1974), p. 25.

14. Brink, G. O., Rev. Sci. Instrum., 37, 857 (1966).

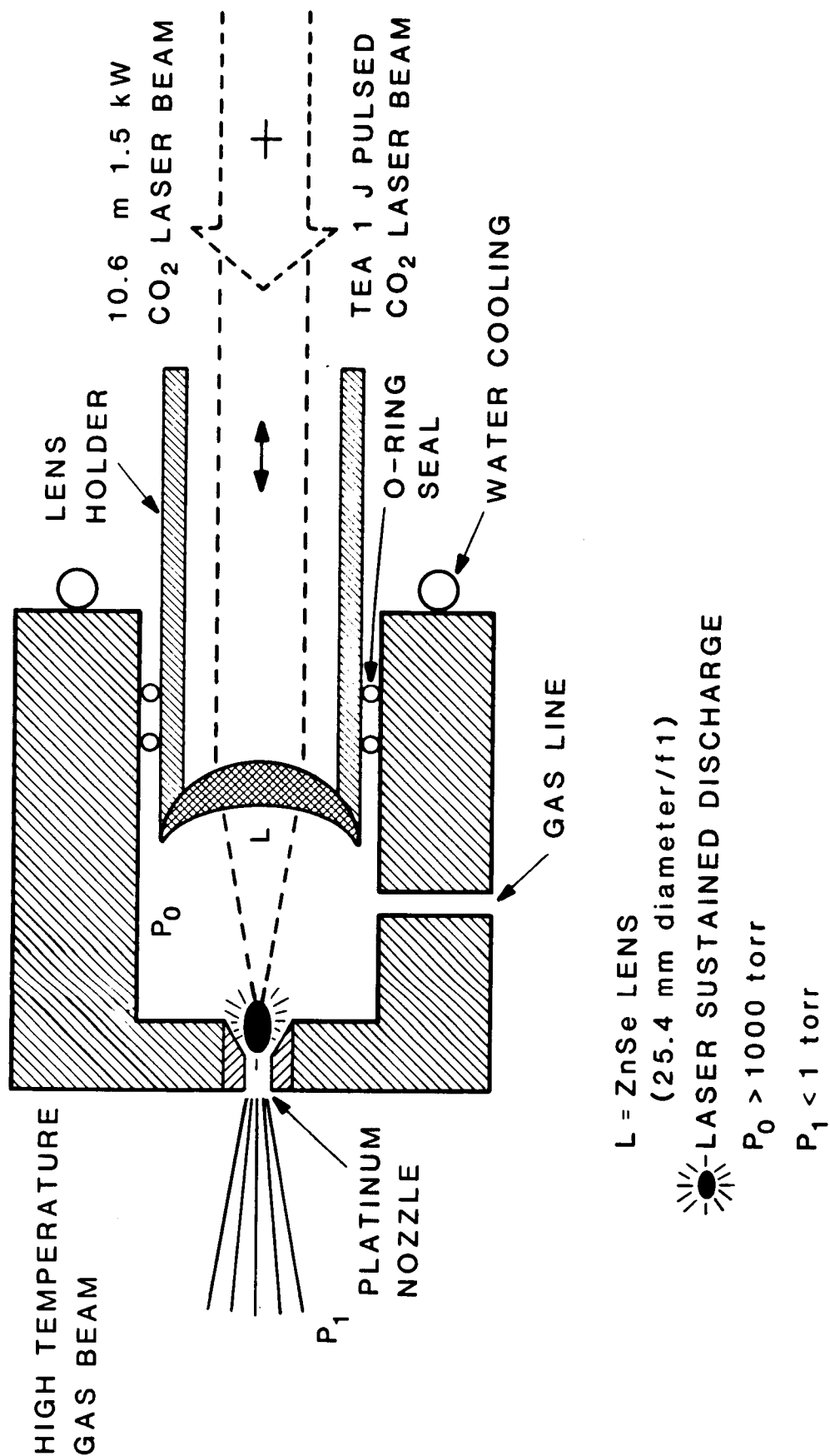15. Femerey, J. K.; J. Vac. Sci. Technol., 9, 108 (1972).

Figure 1. Laser sustained discharge atomic beam source: discharge is initiated using a pulsed (0.5 J) TEA CO_2 laser and sustained with a 1.5-kW CO_2 laser.
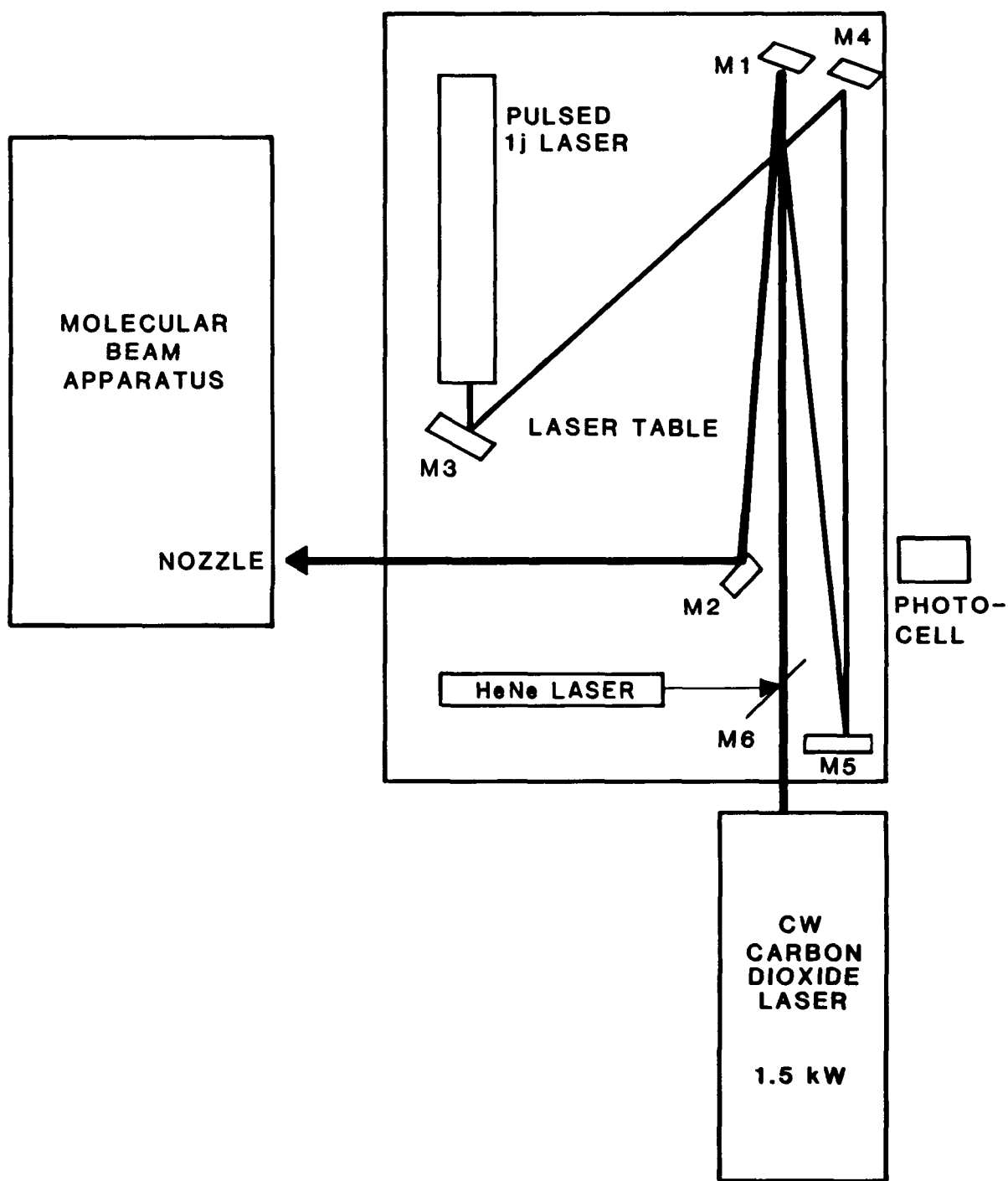
217

Figure 2. Alignment of pulsed and cw CO_2 lasers with nozzle. The 5-cm-diam water cooled mirrors M1 and M2 are used to align both the pulsed and cw lasers with the nozzle. Mirrors M3, M4, and M5 are used to align the pulsed laser with the cw laser. Mirror M6 employs a kinematic magnetic mount to place the HeNe laser beam co-axial to the cw laser beam. When operating the cw laser the mirror M6 is removed. The photocell detects the plasma light emitted from the nozzle assembly and interrupts the cw laser operation if the plasma is extinguished.
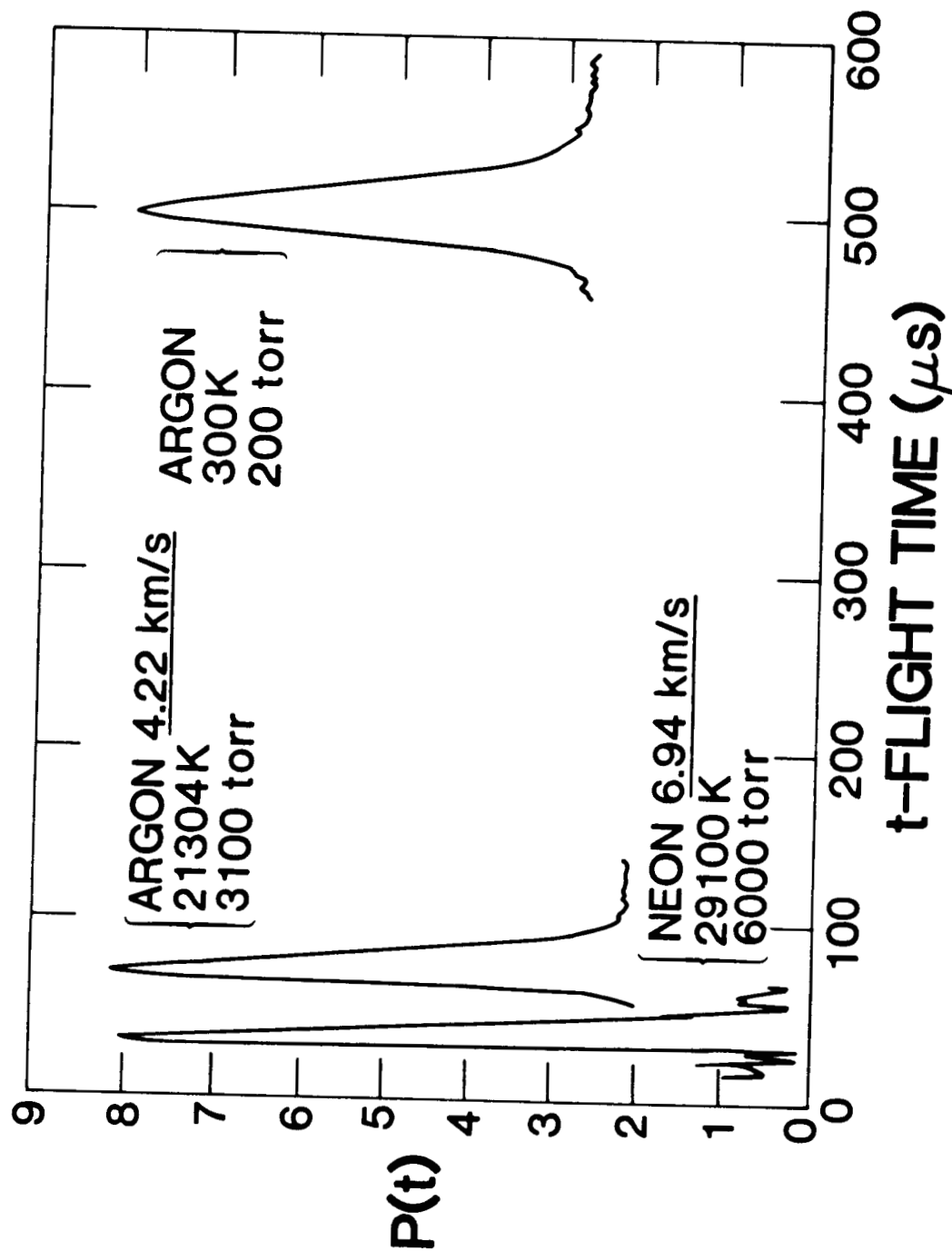
Figure 3. Argon and neon time-of-flight distributions. Flight times have not been corrected for timing mark offset or detector ion flight times.
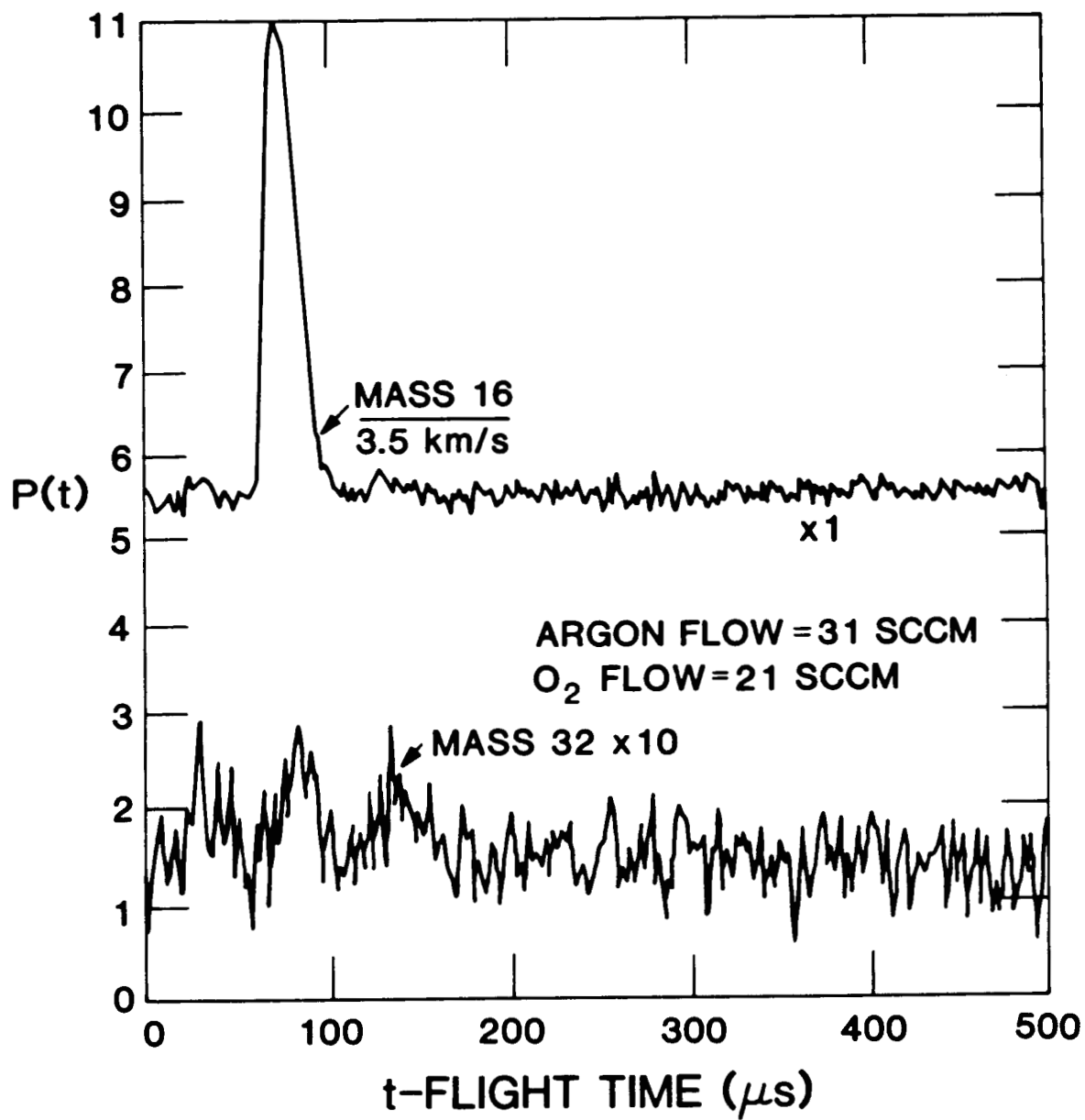
Figure 4. TOF Distribution of mass 16 and 32 using 40% O_2, 60% argon mixture.
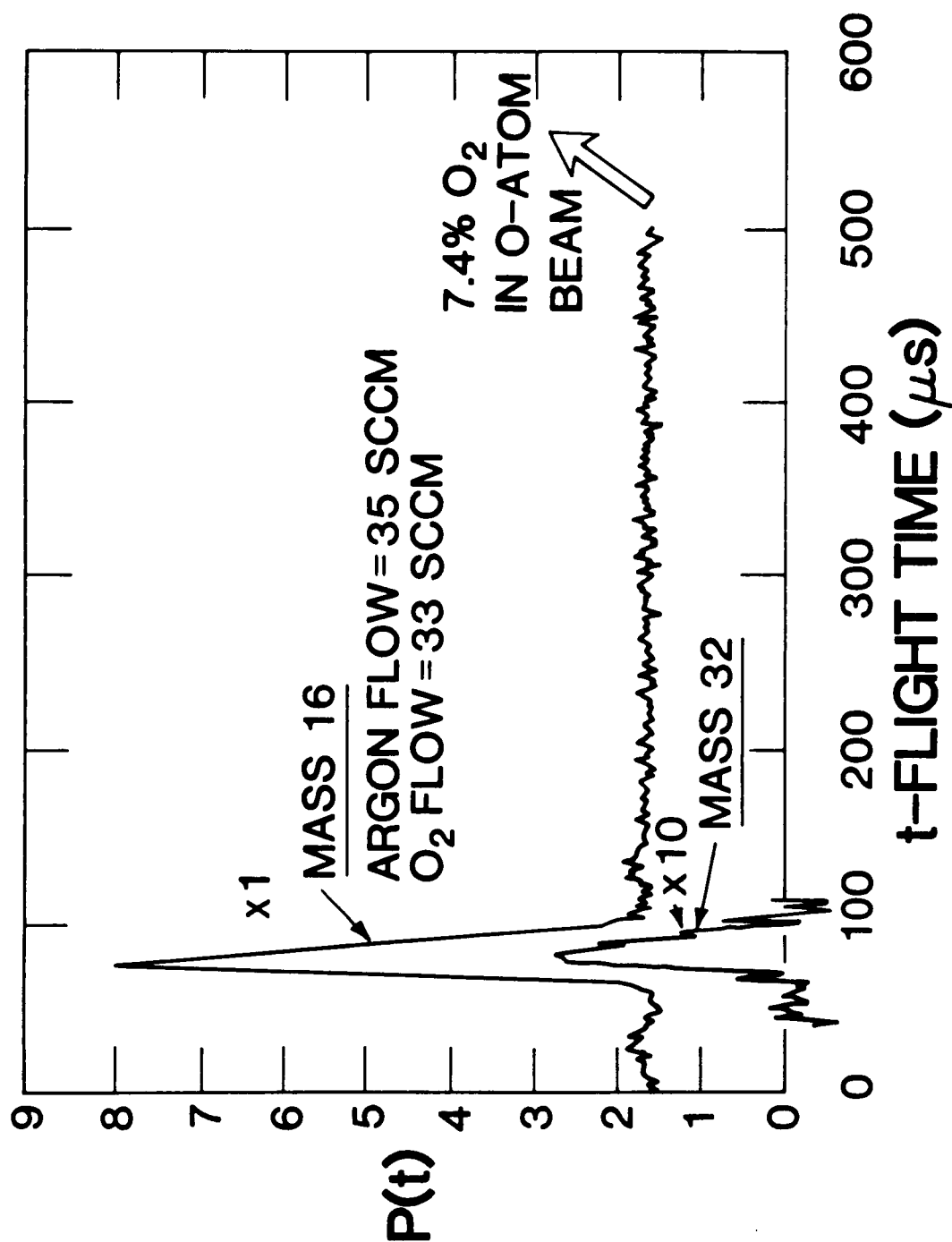
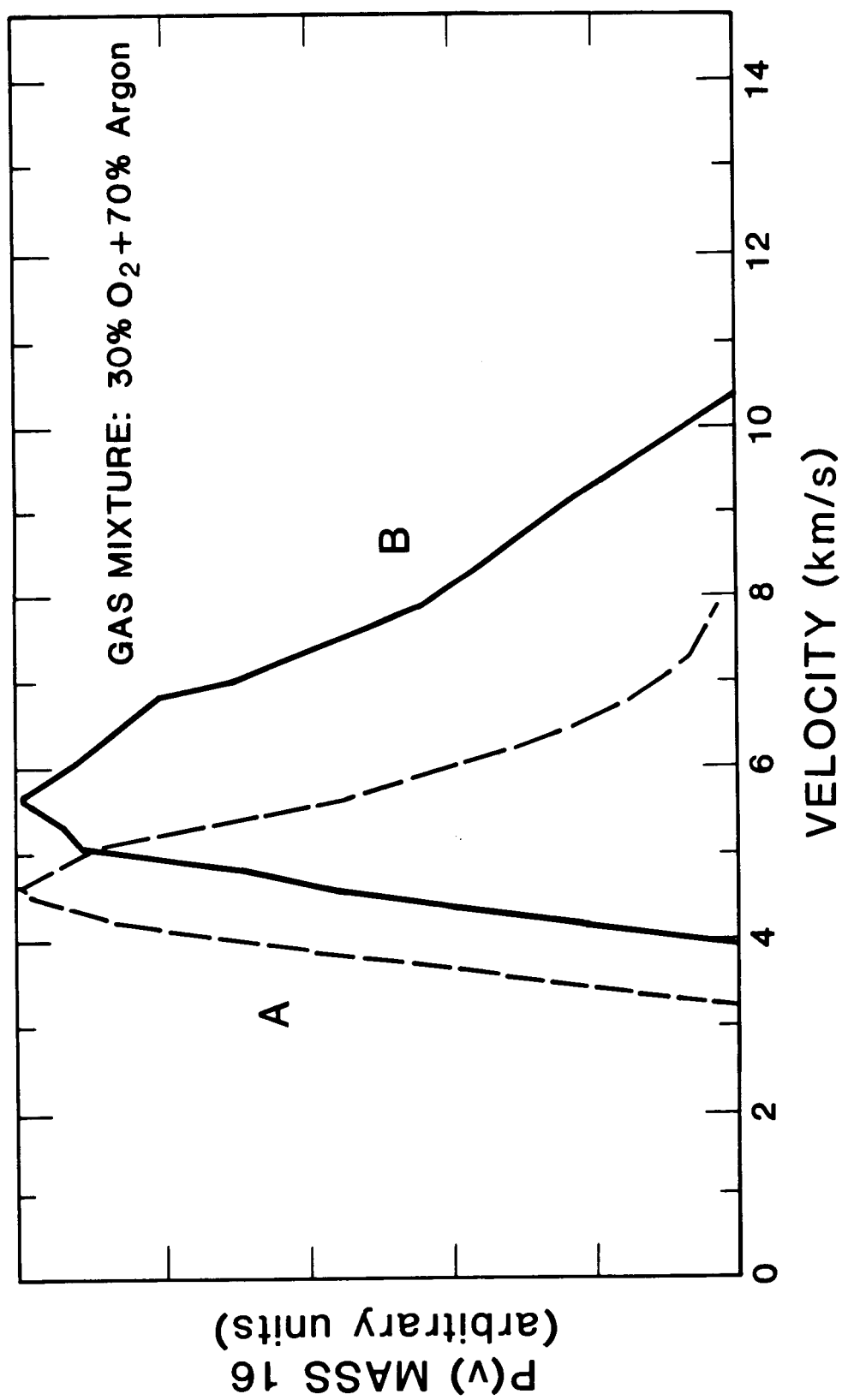Figure 5. TOF distribution of mass 16 and 32 using 49% O_2, 51% argon mixture.

Figure 6. TOF distributions of mass 16 using a 30% O_2, 70% argon mixture. Distribution A was taken with the plasma at the entrance to the nozzle while distribution B was taken with the plasma moved 0.5 mm farther into the nozzle.
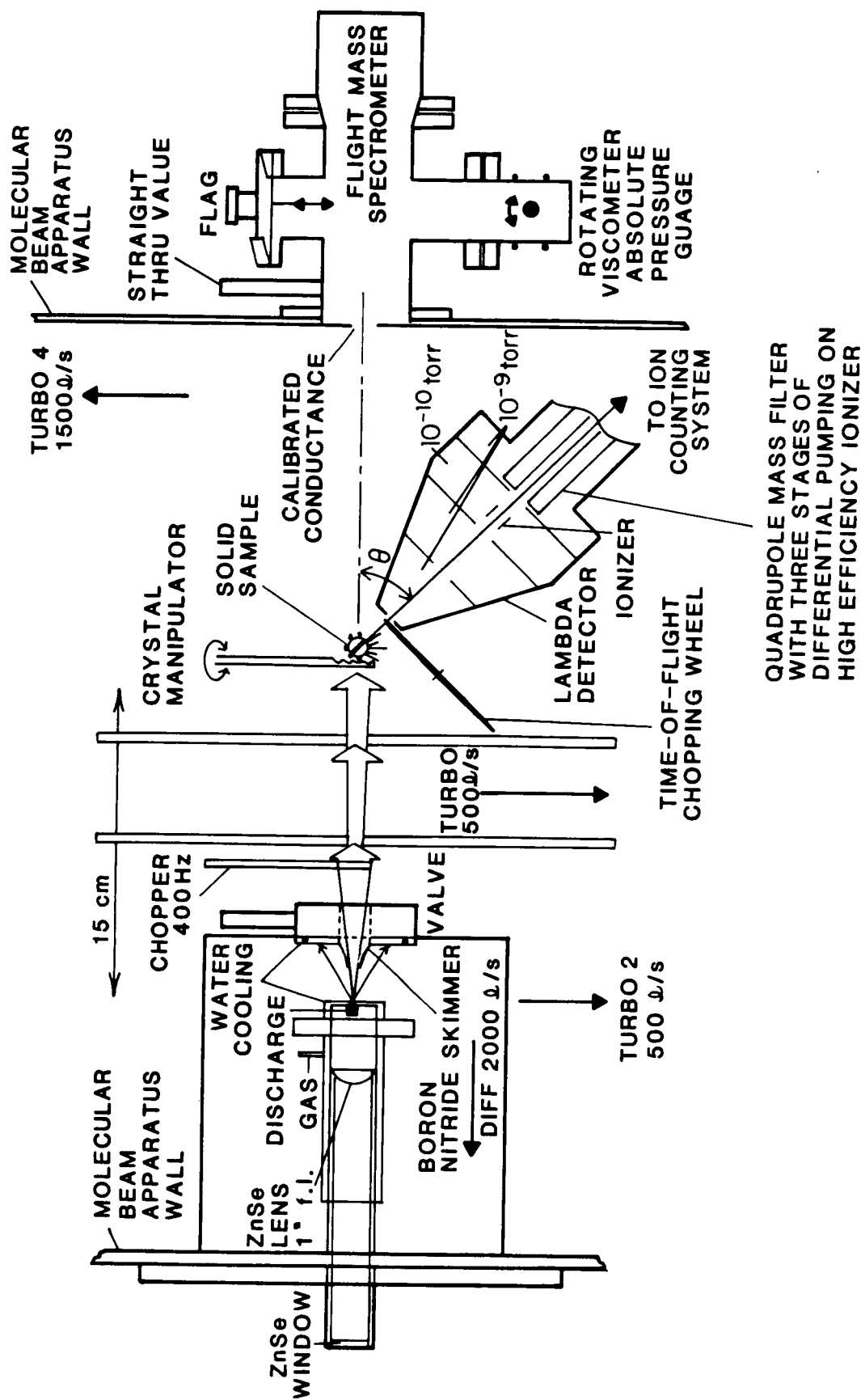
Figure 7. Los Alamos molecular beam dynamics apparatus: shows the central portion of the instrument including the molecular beam source, and movable detector. The detector is an electron bombardment ionizer-quadrupole mass spectrometer suspended from the rotatable lid of the main vacuum chamber and is used for the measurement of angular distributions. Also shown is a time-of-flight chopping wheel that provides 50% transmission efficiency using cross correlation techniques. Pumping of the system is accomplished by a 1500 1/s turbo on the scattering chamber, a 500 1/s turbo on the differential pumping chambers, a 2000 ℓ/s diffusion pump on the nozzle source and ion pumps on the detector.
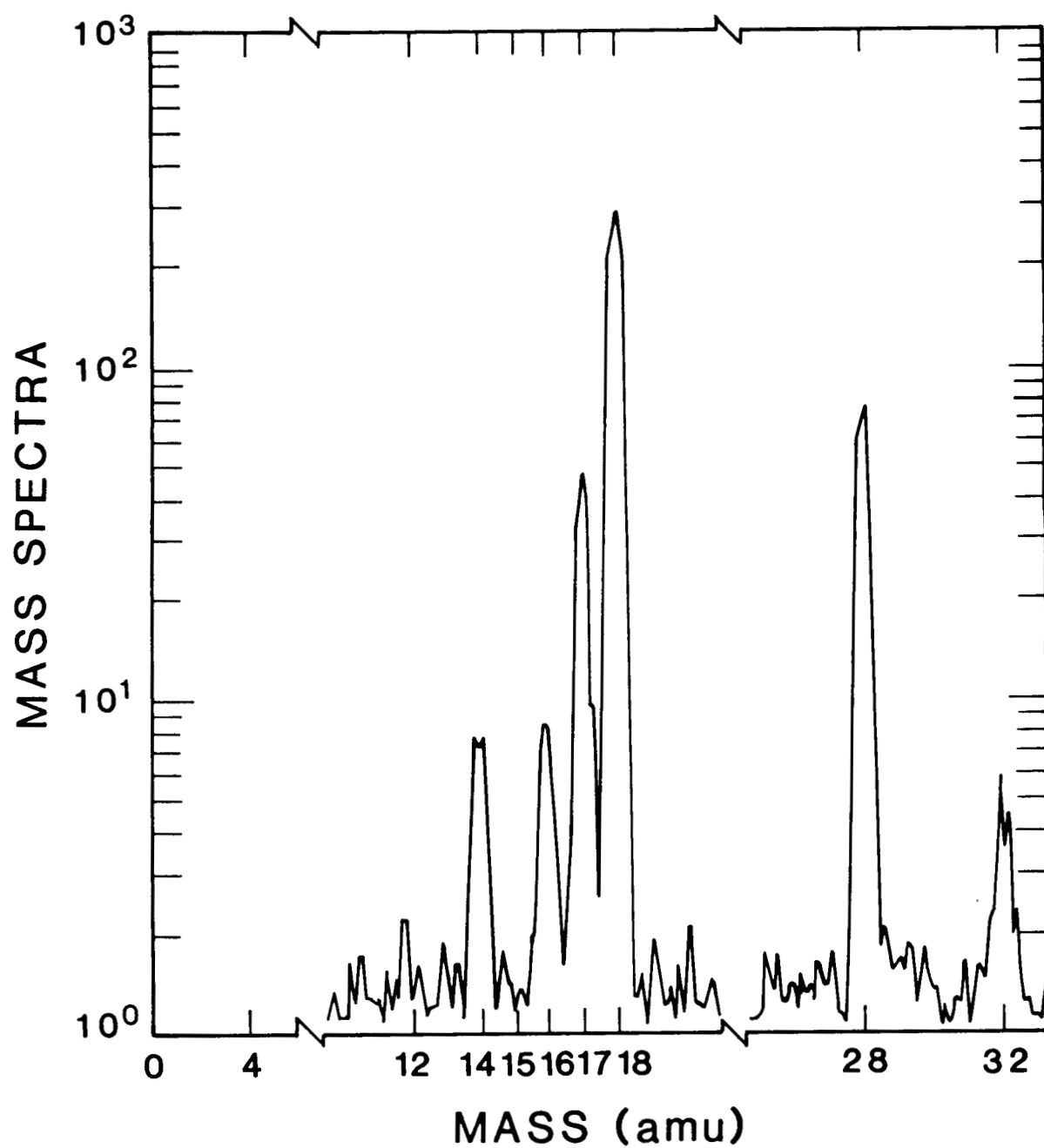
Figure 8. Background (3×10^{-7} torr) mass spectra taken with the AFGL flight mass spectrometer.
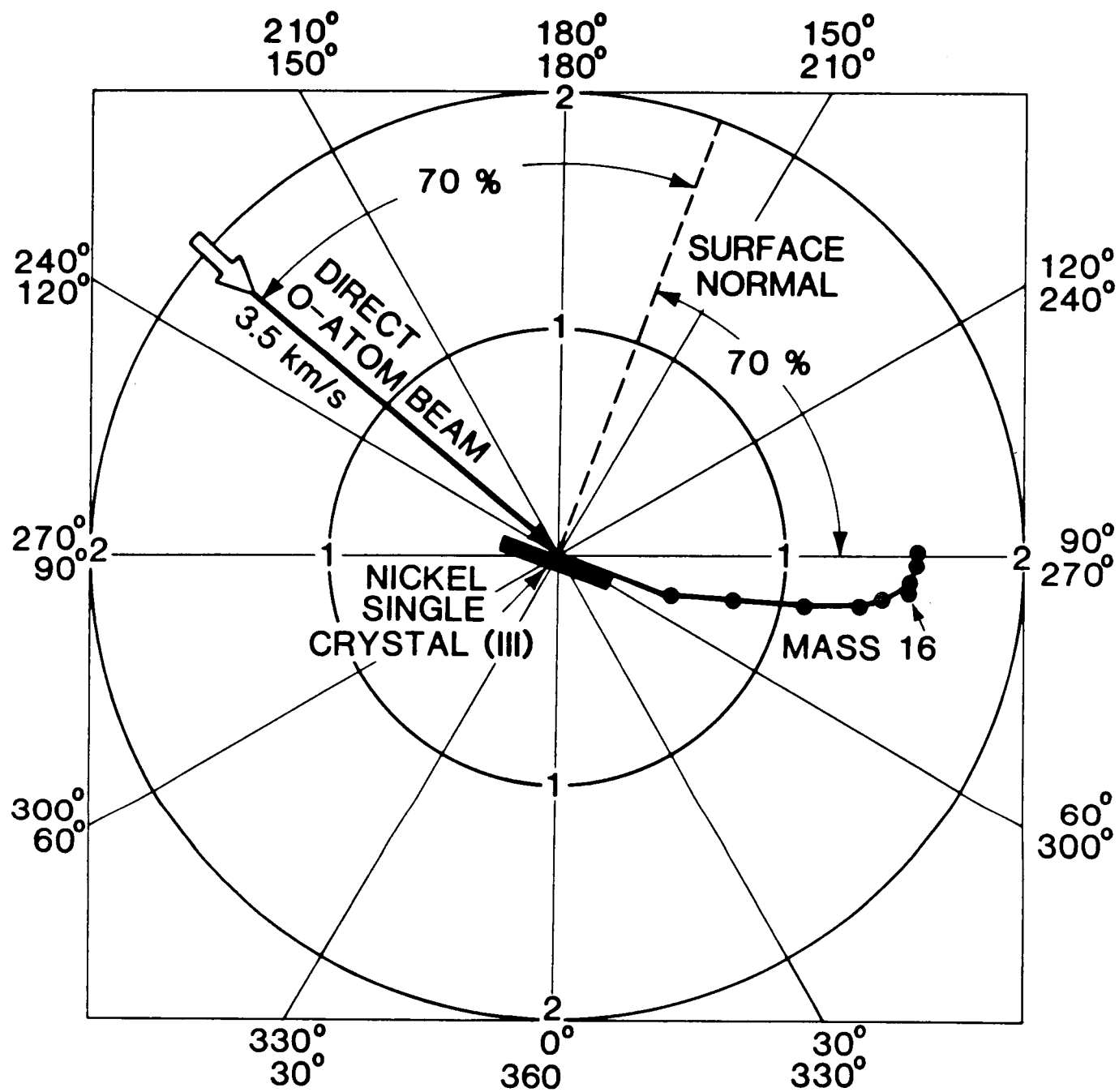
Figure 9. Angular distribution of O-atoms scattered from uncharacterized nickel crystal. Error bars on data points are the size of the plotting symbol. Surface temperature was 300 K.
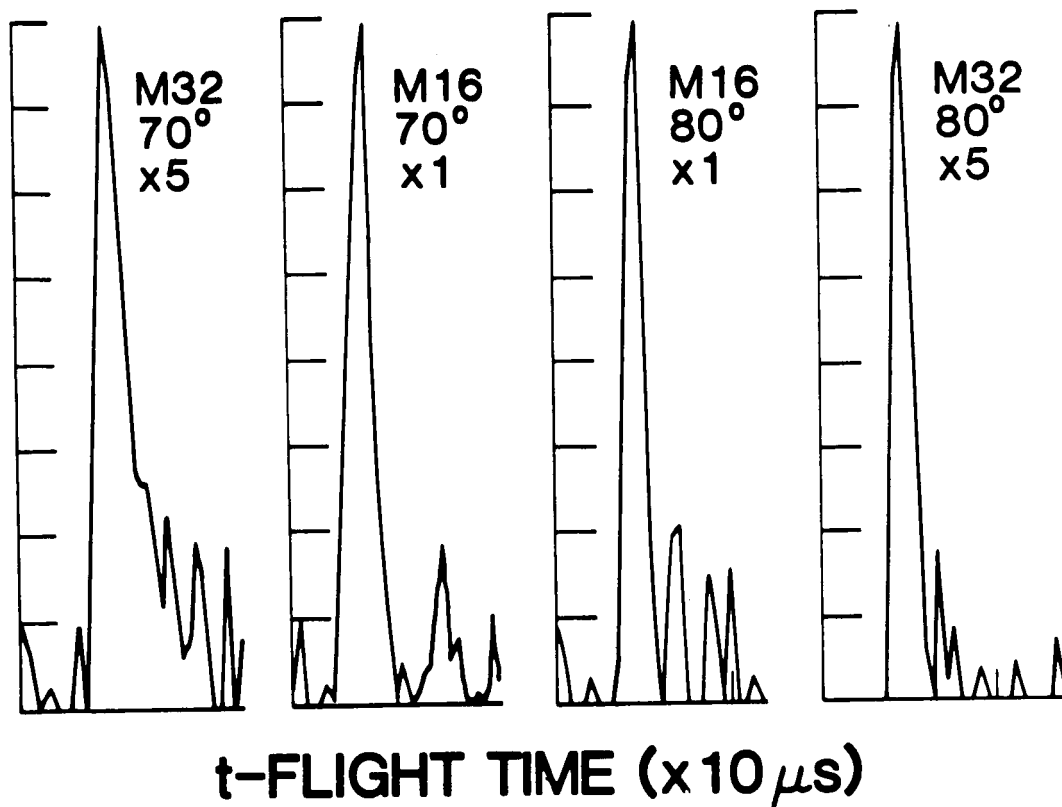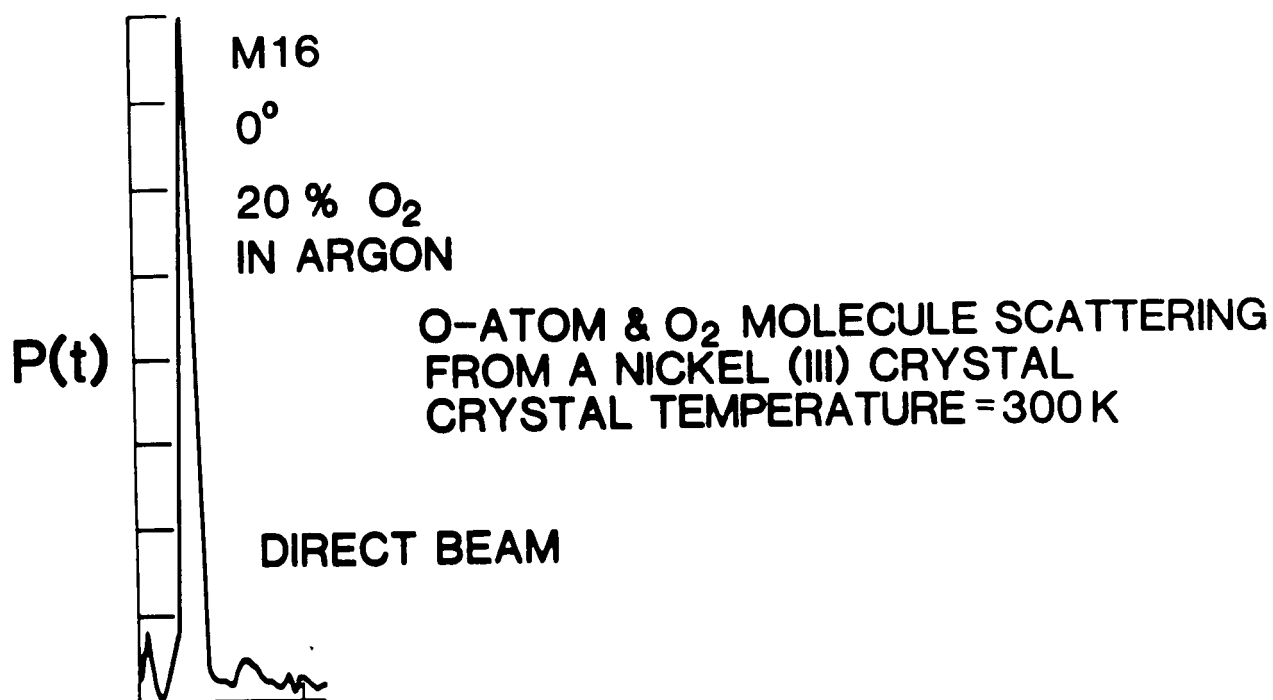
Figure 10. TOF distributions at 70 and 80° from surface normal. The mass 16 distribution when converted to energy indicates roughly 50% of the energy was transferred to the solid.